USE OF A CFD BASED NUMERICAL MODEL TO CALCULATE HEAT TRANSFER IN BOILER SUPERHEATERS PANELS

Rafaela Frota Reinaldo
Universidade Federal de Santa Catarina-Departamento de Engenharia Mecânica
Laboratório de Combustão e Engenharia de Sistemas Térmicos
88.040-900, Florianópolis – SC, Brazil
rafaela@cet.ufsc.br

João Luis Toste de Azevedo
Instituto Superior Tecnico, Dep. Eng. Mecânica
Av. Rovisco Pais, 1049-001 Lisboa, Portugal
toste@navier.ist.utl.pt

Edson Bazzo
Universidade Federal de Santa Catarina-Departamento de Engenharia Mecânica
Laboratório de Combustão e Engenharia de Sistemas Térmicos
88.040-900, Florianópolis – SC, Brazil
ebazzo@emc.ufsc.br

Abstract. *Most unplanned outages in the Jorge Lacerda Power Plant, situated in Capivari de Baixo-SC, are due to tube failures in the boiler. Historical records and metallographic analysis indicate that the working metal temperature of the tubes of the final superheater and reheaters of the utility boiler is higher than the recommended value. The high temperature level of the tubes is the main cause of the tube failures by creep and is an important factor determining the remaining life-time of the tube bundles. This work presents the simulation of the combustion, flow and heat transfer of the utility boiler furnace to determine the metal temperature of the final superheater and reheater. The tube metal temperature is calculated taking into account local convective and radiative heat transfer. This calculation procedure is an extension of the Computational Fluid Dynamics based model for pulverized coal combustion already extensively used at Instituto Superior Tecnico. Comparisons are made between the calculated and measured values of metal heat transfer and the temperature distribution among the tube bundles. Simulations are presented for two different operational conditions in order to analyze theirs influences in the metal temperature.*

Keywords. *utility boiler, superheater, computational fluid dynamics, pulverized coal.*

1. Introduction

The current electrical power generating capacity installed in Brazil is about 74 GW. The thermal power plants generate 17% of this amount, most based on the Rankine cycle using coal-fired boilers. The Brazilian electric system is strongly dependent on the water levels of the reservoirs, once it is also strongly based on the hydropower generation plants. Recently, a continuous absence of rain led the reservoirs to critical water low levels. This situation forced the Brazilian government establishing a global emergency plan and the population reducing the use of electrical energy.

The motivation of this work is the increase of availability of existing thermal power plants in order to minimize the risk of new black-outs and to attend the growing demand of energy in Brazil. Following this purpose the Tractebel Energy Company is supporting an investigation focusing the operational trustworthiness of the power plant units of Jorge Lacerda in cooperation with the Federal University of Santa Catarina (UFSC). Among different tasks, a complete review has been performed of the original material selection, failure history, past maintenance, and other critical information, in order to determine if there are any operational conditions that impact the superheater and reheaters life. Long-term creep failures can normally be attributed to the localized high temperatures resulting from poor boiler design, operation at off-design conditions, burner-related problems, etc. The failures in the tubes of superheaters and reheaters are the main cause of the unplanned outages in coal-fired utility boilers in Brazil (Felippe and Santo, 1998). Some poor design problems can be due to steam flow problems as a consequence of poor header designs or gas temperature imbalances resulting from firing arrangements or gas temperature stratification problems caused by wall firing configurations. Practically all boilers operate with some form of temperature distribution problem, resulting in the tubing suffering from accelerated creep damage accumulation. About 50% of failures are due to the creep phenomenon that occurs under conditions of high temperatures. The metal temperature measurement of the tube bundle is important for the determination of the remaining tube life (EPRI, 1985). Replacement of tubing is most often done as a result of failures at the hottest locations. Redistributing or smoothing out the temperature profile across the unit will reduce the temperature at hot spots while increasing temperature at the cooler locations. This will have the benefit of significantly increasing the life of the tubes. It has been shown that most amount of tubing is replaced prematurely. Minimizing the unplanned outages or tube replacements, increasing the tubing life, and decreasing the failure rate will reduce the maintenance and capital costs. That is the main objective of this work. Additional to the experimental measurement of the metal tube temperature, it is important to predict with accuracy the metal tube temperature under different operational conditions. With this intention, a calculation procedure was developed at Instituto Superior Tecnico and added to a Computational Fluid Dynamics (CFD) based model for pulverized coal combustion already extensively used. Coimbra et al (1994) and Xu et al (2000) analysed the influence of operating conditions on furnace performance. The numerical model was also used to assist the design of furnaces using reburning by Coelho et al (1999) for an existing furnace and Toledo and Azevedo (2003) for new furnaces including different types of boiler design that were compared. Important parameters that can be analysed using the numerical model are gas mixing, heat transfer, particulate matter combustion and NOx formation from a post-processor model.

The application of CFD models to the boiler furnace was extended to the convection section of a parallel path boiler by Coelho (1999a) coupled with the calculation of radiation heat transfer in the enclosures between the tubes as presented by Coelho (1999b). This model application was performed using a two dimensional approach taking into consideration average properties obtained from a three dimensional numerical model simulation to the boiler furnace. The treatment of radiation heat transfer in the spaces between the superheaters panels is adopted here in the three dimensional numerical model to simulate the heat transfer process. This type of approach is also used in monitoring heat transfer models to boilers as described in Azevedo (2003).

The present paper describes in summary a description of the boiler in section 2 and the adaptations done in the CFD based model in section 3. Section 4 presents results from the application of the model with emphasis on the temperature distribution in the cross section of the furnace exit.

2. Description of the problem

The utility boiler #6 of the Jorge Lacerda Power Plant produces superheated and reheated steam for a 125MWe capacity generator. A sketch of the boiler is shown in Fig. (1)

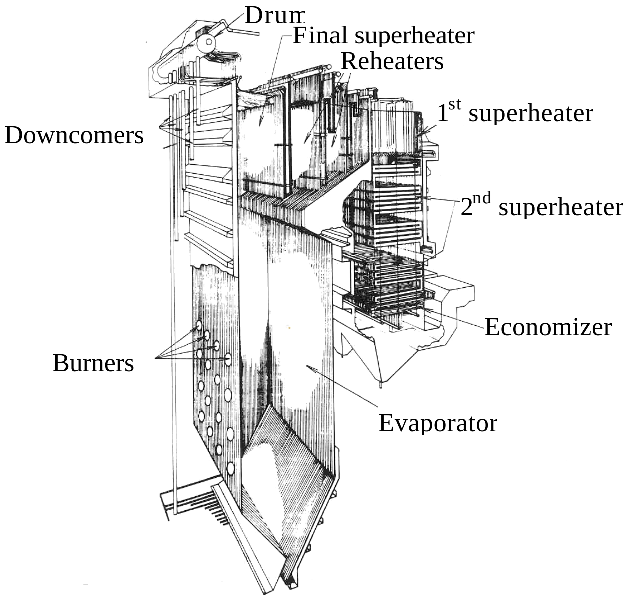

Figure 1. Utility boiler.

The utility boiler consists of a natural circulation system with external downcomers and tube wall membranes connected to the same boiler drum. The furnace is front wall fired with sixteen burners divided in four rows corresponding to four pulverised coal mills. Each wall burner consists of several concentric inlets with two main annulus inlets, the inner inlet with 0.50m diameter with feeding coal transported by primary air, surrounded by another annulus with 1.02m for secondary air. The combustion gases flow upwards in the furnace and after the boiler arch through the final superheater and reheaters, which are located in the exit of the combustion chamber. Then the gases flow down through the primary superheater, secondary superheater and economizer that are located in the convection chamber.

The final superheater is composed of 40 panels with transversal pitch of 300mm. Each panel has seven tubes in the flow direction with external diameter equal to 31.8 mm and 60m pitch. The reheater is composed of 78 panels with a transversal pitch of 150mm. Each panel has four tubes with external diameter equal to 44.5 mm and a longitudinal pitch of 70 mm. The position of the panels is shown in Fig (2).

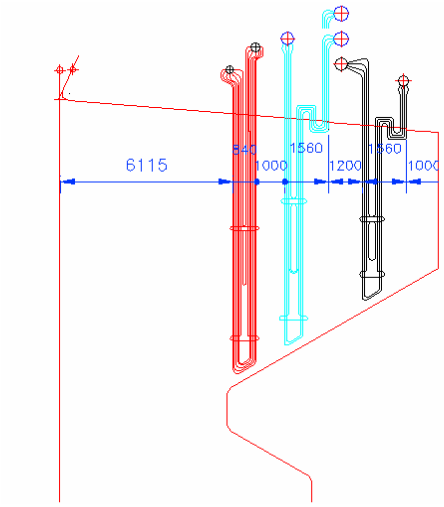

Figure 2. Final superheater and reheaters.

The metal temperatures of the final superheater are measured by thermocouples fixed near the steam collector. Large temperature differences are observed between the central region and near the furnace walls. The non-uniform temperature profile occurs mainly in the right side of the boiler, leading to values higher than 810 K, affecting the integrity of the metal, causing creep and reducing the residual tube life time. A metallographic study of the final superheater metal is reported in the work of Bernardini *et al.* (1999), showing that the degradation of the metal is caused by the creep phenomenon resulting from the high working temperature.

3. Methodology

The numerical model of the combustion chamber is based on the calculation of the turbulent flow based on balance equations for mass, momentum components and turbulence quantities: turbulent energy and its dissipation. These balances to the continuum gas are performed in an Eulerian base using a similar discretisation procedure for all, except for the continuity equation that is treated by the Simple algorithm to calculate pressure. Gaseous combustion is modelled using the mixture fraction and its variance based on a clipped Gaussian distribution. Gas temperature is calculated from an energy balance, considering the heat exchanged by radiation based on the discrete transfer method (Lockwood and Shah, 1981). The mixture fraction and energy balances consider source terms due to the presence of the particles that are simulated using a Lagrangian approach. The momentum and heat balance to the particle is calculated along representative particle trajectories, considering instantaneous gas properties from a stochastic model. Empirical models are used to describe coal particle devolatilisation and char combustion in sequence. More details of the general approach of pulverized coal boilers models are presented in the work of Eaton *et al.*(1999) or can be found in Toledo and Azevedo (2003).

The energy balance in the tubes of the heat exchangers is made taking into account the convection and the radiation heat transfer from the combustion gases to the surface of the tube, conduction in the deposits and metal tube and convection to the steam inside the tube. Considering the segment S, of the tube T at the panel P of a heat exchanger, shown in Fig.(3), the heat flux transferred q(W/m^2), from the gas to the tube is

$$q = h_g\left[T_g(I,J,K) - T_w(S,T,P)\right] + \varepsilon_t\left[G_t - \sigma T_w^4(S,T,P)\right] \tag{1}$$

expressing the sum of the convection and radiation heat transfer mechanisms. T_g (I,J,K) and T_w (S, T, P) are the local gas temperature and the external wall temperature respectively and h_g is the convection coefficient calculated using the correlation of Zukauskas (1998). The radiation contribution is calculated from the difference between the irradiation G_t and the emissive black body power $E_{b,t}$ multiplied by the tube surface emissivity ε_t.

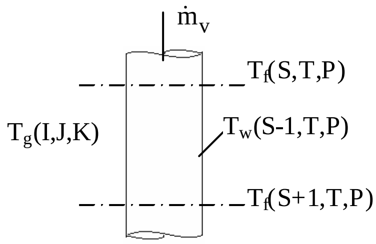

Figure 3. Temperatures on a section of tube.

The irradiation in the p row of tubes is obtained using a simplified formulation based on the zone method, presented in Coelho (1999b):

$$G_{t,r} = \frac{\left[\tau_g F_{ht} S_T/(\pi D)\right]\left[(1-F_{ht})^{r-1}\left(G_{in,1}-\varepsilon_t E_{bt,r}\right)+(1-F_{ht})^{N_L-r}\left(G_{in,2}-\varepsilon_t E_{bt,r}\right)\right]+\varepsilon_t E_{bt,r}\tau_g+\varepsilon_g E_{bg}}{1-\rho_t\tau_g+\left[\rho_t\tau_g F_{ht} S_T/(\pi D)\right]\left[(1-F_{ht})^{r-1}+(1-F_{ht})^{N_L-r}\right]} \quad (2)$$

where τ_g and ε_g are the transmissivity and emissivity of the gas respectively, ρ_t is the reflectivity of the tube, F_{ht} is the view factor of a infinite plane to a row of tubes, S_T is the transverse pitch, D is the external diameter, N_L is the total number of rows, $G_{in,1}$ and $G_{in,2}$ are the radiative energy incoming to the region of the heat exchangers crossing the fictitious planes 1 and 2 situated in the front and rear sides of the heat exchanger, respectively, as show in Fig.(4).

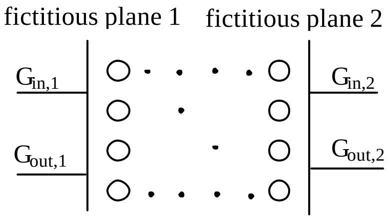

Figure 4. Incoming and outgoing radiative energy across the fictitious planes.

The value of $G_{in,1}$ for the final superheater is obtained from the calculation of the irradiation onto a fictitious plane 1 using the discrete transfer method. The side of the fictitious plane facing the furnace receives the incident radiation energy incoming from the furnace, G_{in1}, minus the outgoing radiative energy crossing the fictitious plane, G_{out1}, so, the calculation of the heat flux onto the fictitious plane is iterative. The values of $G_{out,1}$ of the final superheater and $G_{in,1}$ for the reheater are determined by the model for the radiative transfer in tube bundles presented in details in Coelho (1999b). The value of $G_{in,2}$ for the reheater is estimated as the emissive power of a black body with the gas temperature after that reheater. This can be refined considering further rows of panels and cavities.

The tube external surface temperature is calculated from the equality between the absorbed heat and the heat transferred, from the tube to the steam:

$$q = U_{sf}\left[T_w(S,T,P) - \frac{T_f(S,T,P)+T_f(S+1,T,P)}{2}\right] \quad (3)$$

where $T_f(S,T,P)$ is the inlet fluid temperature. U_{sf} is the tube to steam heat transfer coefficient and is calculated by:

$$U_{sf} = \left[R_f + \frac{D}{2k}\ln\left(\frac{D}{D_i}\right) + \frac{D}{D_i}\left(R_{Ox} + \frac{1}{h_i}\right)\right]^{-1} \quad (4)$$

where h_i is the internal convection coefficient and D and D_i are the external and internal tube diameter. R_f and R_{ox} are the heat transfer resistances respectively due to slagging and fouling and of the oxide layer in the internal side. R_f is considered as zero and R_{ox} is equal to 0.0005 m^2 K/W, this value is calculated based on the maximum measured oxide layer thick, equal to 0.3mm with thermal conductivity of 0.59 W/(m K).

The steam temperature is calculated from the enthalpy calculated from an energy balance based on the upstream value:

$$h_{f(S+1)}\left[T_f(S+1), P_f(S+1)\right] = h_{f(S)}\left[T_f(S), P_f(S)\right] + qA_S/\dot{m}_S \quad (5)$$

where $\dot{m}_S$ is the steam mass flow rate, $h_{f(S)}$ is the enthalpy of the steam in the sector S , P_f is the pressure of the steam and A_S is the external area of the tube. No pressure drop was considered at this stage.

A numerical simulation was performed for the standard operational condition of 125MWe, with the 1^{st}, 2^{nd} and 3^{rd} rows of burners operating with 23 kg/s of pulverized coal with 164.8 kg/s of air. In this condition the steam production is 395 ton/h at 788K at the pressure of 121.6 bar in the final superheater and 27.5 bar in the reheater. The inlet temperature is 700 K in the final superheater and 660K in the reheater. Two swirl burners' arrangements have been tested, and are denoted by case A and case B as shown in Fig. (5)(a) and (b), respectively.

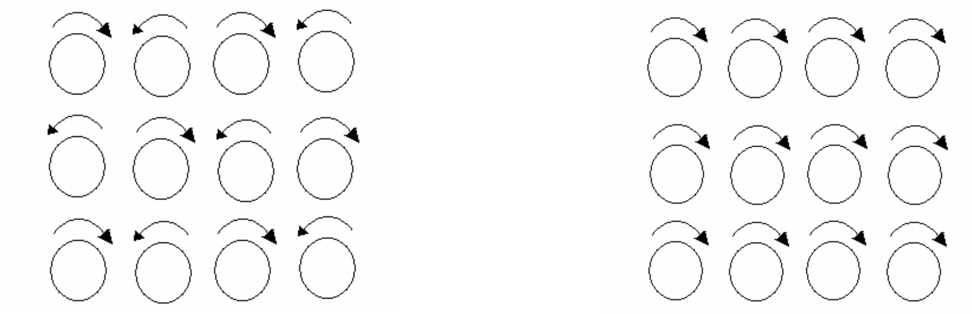

(a) case A (b) case B

Figure 5. Swirl burners' arrangements.

The numerical results are obtained using a non-uniform grid of 40 x 69 x 129 cells for the flow calculations, with finer grids in the burners' zone, and uniform grid of 17 x 12x 40 cells for the radiation heat transfer calculation. About 3000 iterations were required to achieve a converged solution, with an interval of 10 iterations for the call of the calculations of trajectory, radiation and heat transfer in the tubes bundles.

4. Results

The gas temperature and velocity in a vertical plane crossing the first column of burners from the right side are presented in Fig. (6) (a) and (b), respectively. The flow is characterized by the formation of a large recirculation zone at the ash pit region and a deflection of the flow from the burners at the back wall of the furnace. This leads to higher velocities close to the furnace arch where the flow is deflected towards the superheater panels. The location of the main flame region can be identified from the temperature distribution. Following the inlet, larger temperatures are observed at the center of the furnace where most volatiles are burned. The gases are then cooled when deflected towards the furnace exit. As can be observed from this figure at the furnace exit the higher temperature is observed close to the

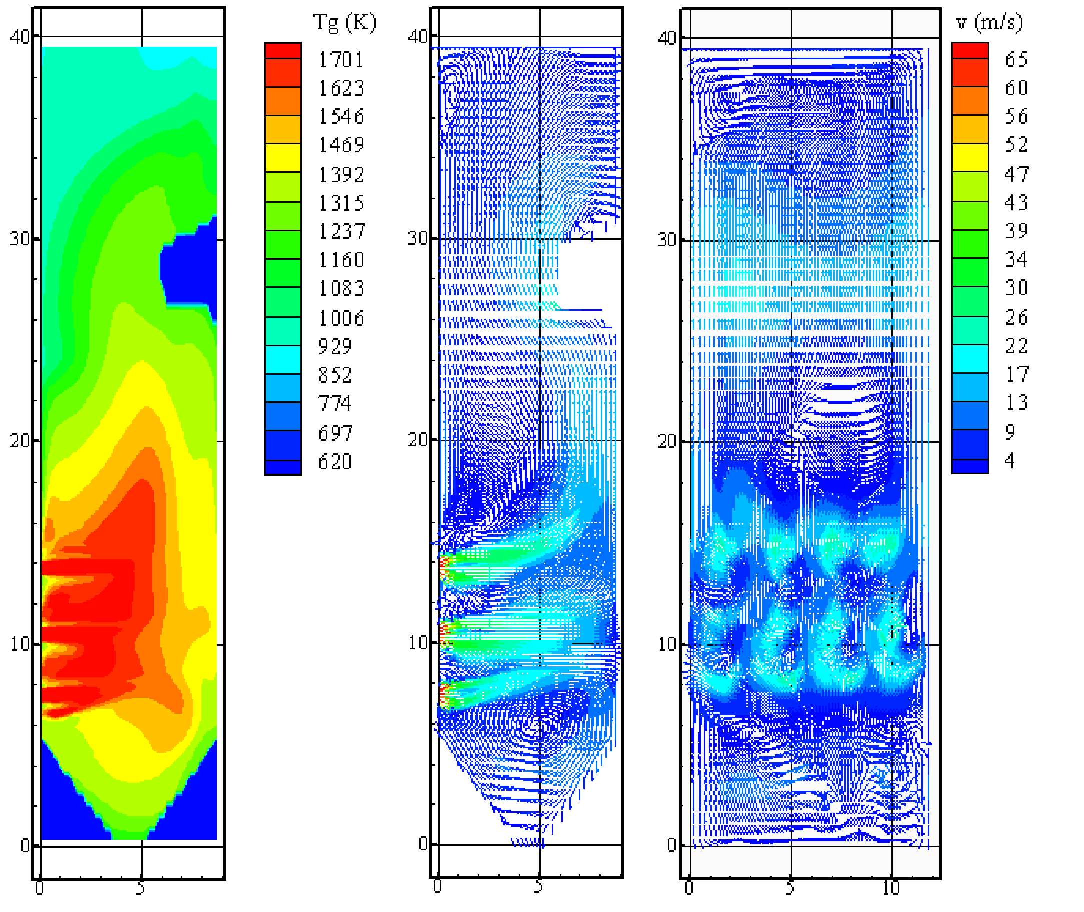

(a) temperature (b) velocity (c) velocity

Figure 6. Gas temperature and velocity in the furnace.

furnace arch. The gas velocity in a plane parallel to the burners, situated 5m from the back-side wall, is presented in Fig. (6) (c), it can be observed a recirculation in the flow in the top-left region. The results shown here correspond to the swirl arrangement B in Fig. (5) that are the actual operating condition of the furnace. Figure (6) (c) shows that the flow is deflected mainly towards the right side of the furnace, forming a recirculation pattern in the top-left region. This is a result of the orientation of the burners swirl and has consequences on the flow and temperature distribution facing the superheater panels as discussed below.

The temperature and normal velocity field in the plane upstream of the final supeheater are shown in Fig. (7) and Fig. (8), respectively. It is observed that the velocity and temperature are larger at the lower section of the superheaters as expected. These figures shows that the higher gas velocity and temperature are observed at the left side of the furnace, although on average the gas temperature is higher in the right side of the furnace. This fact is most accentuated for the case B as a consequence of the orientation of the swirl motion from the burners.

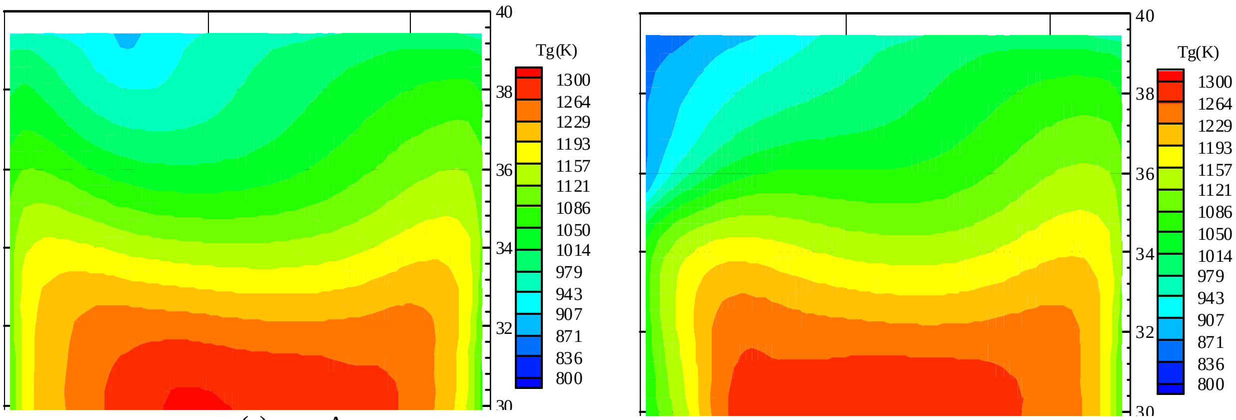

(a) case A (b) case B

Figure 7. Gas temperature in the plane upstream of the final supeheater.

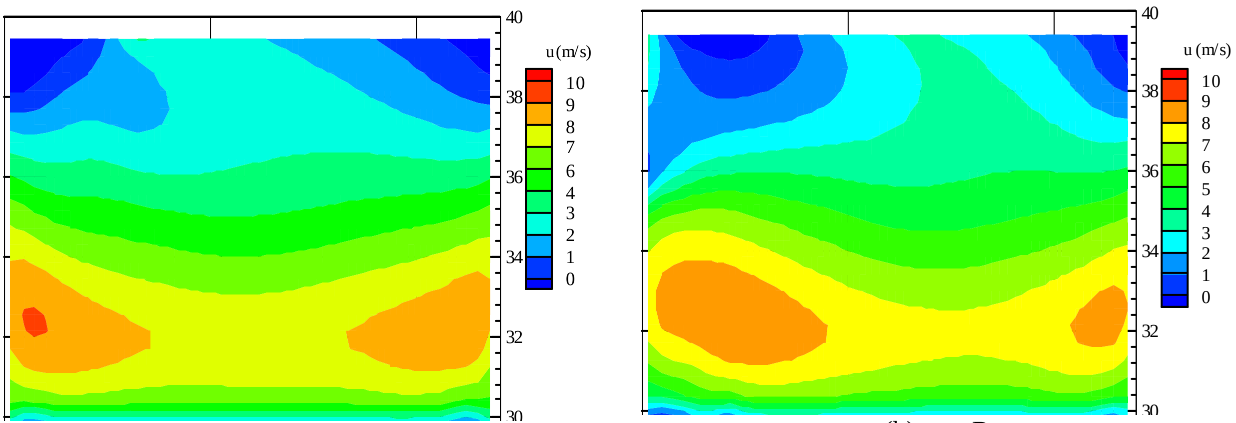

(a) case A (b) case B

Figure 8. Normal velocity in the upstream section of the final superheater.

The irradiation field onto the fictitious plane in front of the final superheater is shown in Fig. (9). As expected larger values are observed at the lower section and decrease along the height. As for temperature, the irradiation is larger on the right side of the furnace. These values are used as boundary conditions for the radiation heat transfer in the superheater panels and were obtained after an iterative procedure with the calculations for the radiation panels.

The predicted temperatures of the wall and the steam in the first row of tubes of the final superheater are shown in Fig. (10) and Fig.(11), respectively. From Fig. (10) it can be observed that the panels situated near the furnace walls have lower metal tube temperatures than the central ones, and the panels on the right side have larger temperatures. The maximum values in this side exceed 810K. The steam temperature shows that the heat extraction is larger in the right side panels. The inlet temperature for the front tubes is already larger at the right side due to the larger heat absorbed in the first descending path in the tubes.

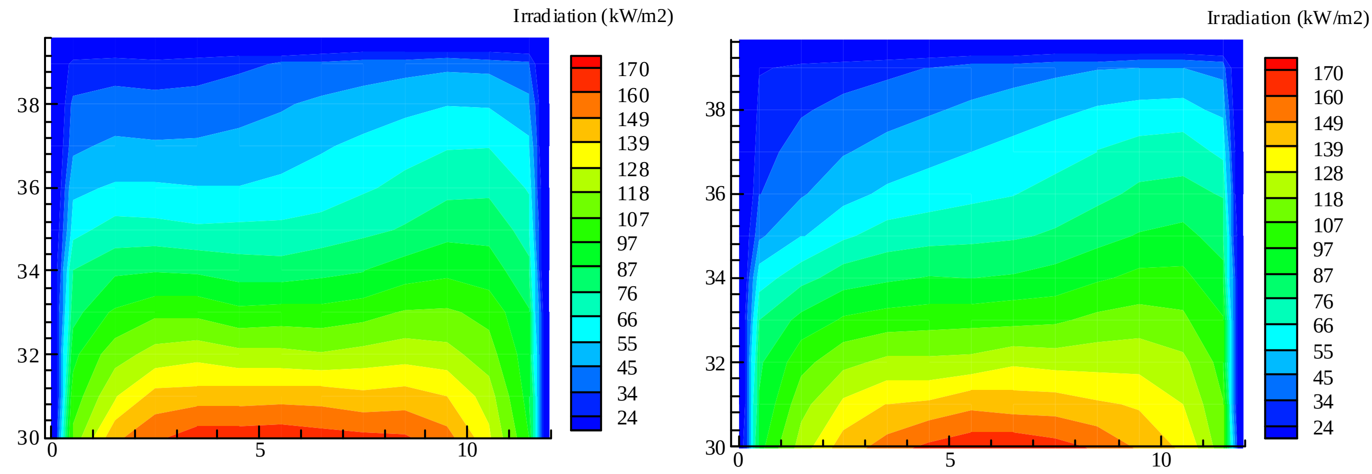

(a) case A

(b) case B

Figure 9. Irradiation onto the fictitious plane of the final superheater.

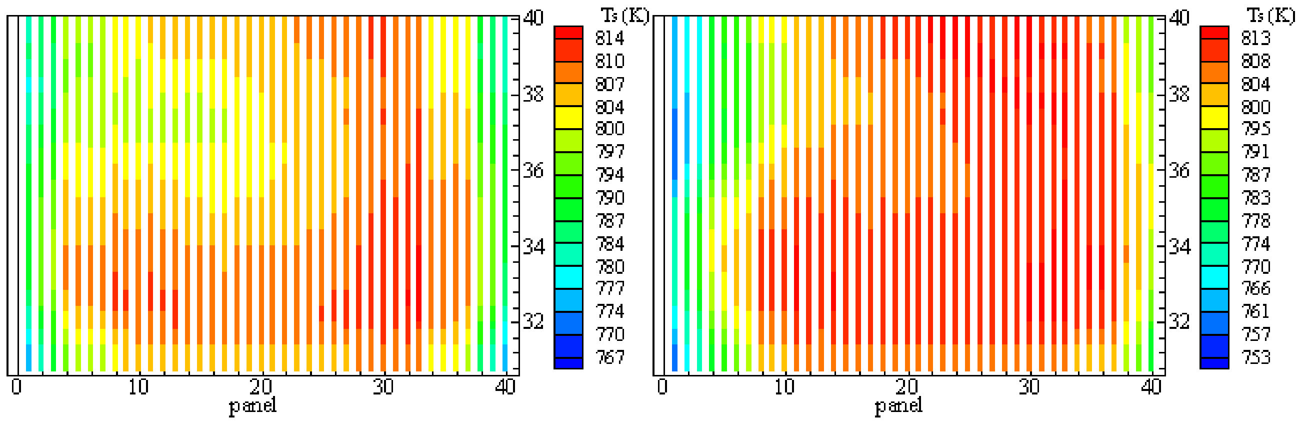

(a) case A

(b) case B

Figure 10. Final superheater wall temperature.

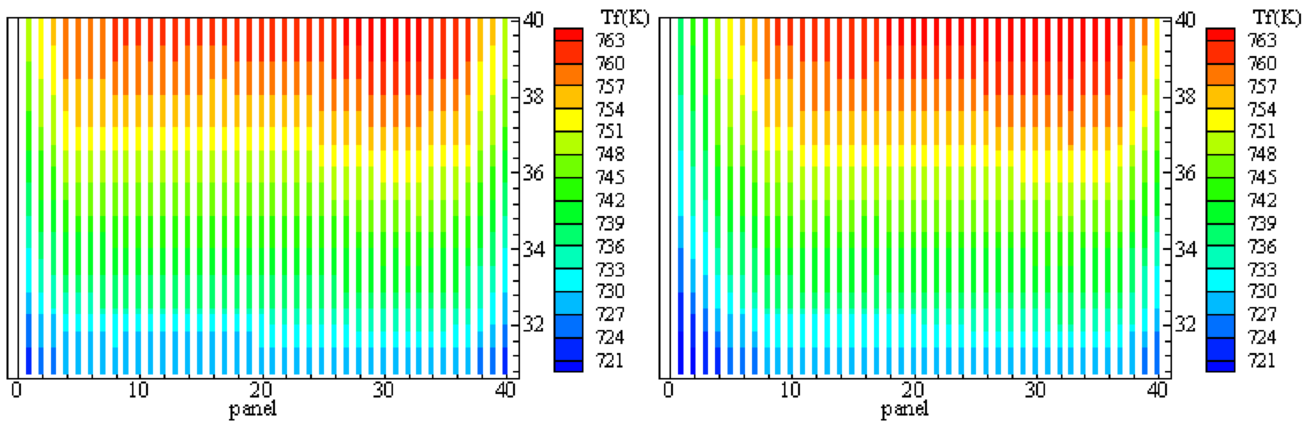

(a) case A

(b) case B

Figure 11. Final superheater steam temperature.

The total amount of heat transferred to the wall furnace and to the panel heat exchangers, calculated and measured by the difference of enthalpy of water/steam in the outlet and inlet sections of these components are presented in Tab. (1). It is also presented the radiative and convective parcels of the transferred energy. The calculated value of heat transferred to the walls is 30% higher than the measured one, an opposite behavior is observed for the superheater and reheater, where the calculated values of heat transferred is 32 and 51% lower than the measured ones. The area of the reheater in the numerical simulations was lower than in the real boiler as some of the panels have an additional tube passage. The area considered in the simulations is 9.8% smaller, partially justifying the relative differences obtained in the simulations.

The higher heat absorption in the furnace walls gives a lower exit gas exit temperature decreasing, in this way, the heat transferred to heat exchangers. A higher value of the calculated heat transferred to the furnace walls suggest that input wall conditions are different from the real ones; a higher emissivity and a lower wall temperature give a more effective heat transfer. The radiation is the most important mode of heat transfer in the furnace. It can be also observed, for the heat exchangers, that the parcel of energy transferred by radiation is higher for the superheater, due to the direct contribution of furnace irradiation while the relative contribution of radiation for the reheater is lower.

Table 1. Heat transferred to the heat exchangers.

Heat exchanger	Q_{total} (MW) measured	Q_{total} (MW) calculated	$Q_{radiative}$ (MW)	$\frac{Q_{radiative}}{Q_{total}}$ (%)	$Q_{convective}$ (MW)	$\frac{Q_{convective}}{Q_{total}}$ (%)
Furnace walls	176.9	230	205.7	89	24.3	11
Superheater	27.6	18.7	10.0	54	8.7	46
Reheater	30.8	15.2	4.4	29	10.8	71

The calculated and measured gas and steam outlet temperatures are presented in Tab. (2). It can be observed that the calculated gas temperatures are lower than the measured ones, as commented before; the higher value of heat transfer to the furnace walls gives a lower value of gas temperature. It can also be observed that the calculated outlet temperatures is lower than the measured ones, since the heat transferred is sub estimated.

Table 2. Calculated and measured outlet temperature of the heat exchangers.

Position	T (K) calculated	T (K) measured
Furnace exit	1119	1397
After superheater	1091	1292
After reheater	1037	1148
Superheater outlet	760	788
Reheater outlet	726	788

The values of the tube temperature near the outlet section are showed in Fig. (12). The predicted values of metal temperature are very similar, however a more uniform temperature distribution is observed for the case A than for the case B. The predicted values of the metal temperature are in agreement with the measured values, the average difference between them is about 2%.

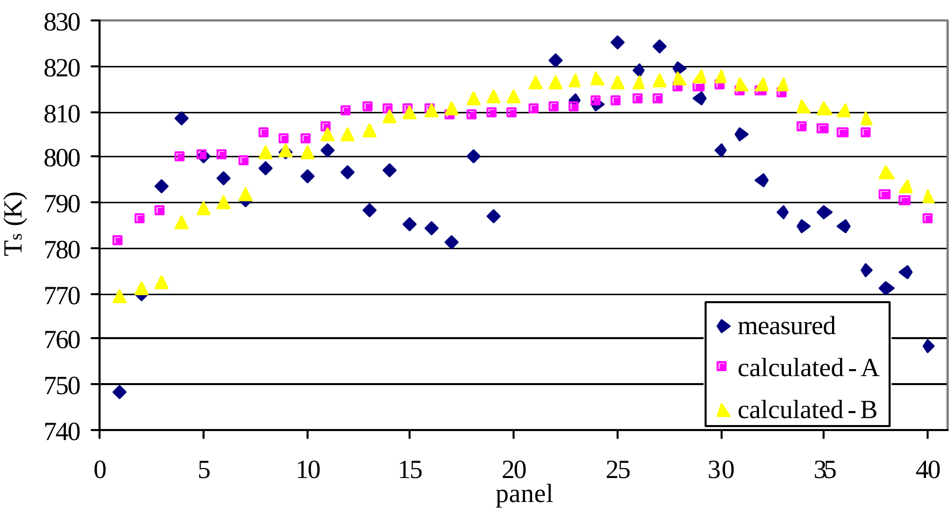

Figure 12. Superheater metal temperature.

5. Conclusions

A methodology to predict the metal and steam temperature in tube bundles of utility boilers is presented. Two different swirl arrangements have been tested. The outlet steam temperature, as well the radiative and convective parcels of heat transferred are independent of the swirl arrangement. The radiation is the most important mode of heat transfer in the furnace, with a contribution of 89%. In the final superheater 54% of heat is transferred by radiation, most part due to the irradiation coming from the furnace. In the reheater the convection contributes with about 71% of the heat transferred, being the most important mode of heat transfer in this section. The estimated amount of heat transferred to the furnace walls is higher than the measured value; which suggests that the input wall conditions (e.g. emissivity and thermal resistance) are different of the actual ones. The overestimation of the heat transferred to the furnace wall results in lower exit furnace temperature, thus lowering the heat transferred to the tube panels. A sensitive analysis is planned in order to determine how the furnace and tube walls conditions affect the results. The predicted values of metal temperature are in agreement with the measured values and a more uniform temperature distribution is observed for the case A.

6. References

Azevedo, J.L.T., 2003, "Implementation of Heat Transfer Monitoring Systems in Solid Fuel Fired Boilers", This Conference.

Coelho, L.M.R., Carvalho, M.G., Pasini, S., Antifora, A., Schnell, U. and Hesselman, G., 1999, "Numerical Modelling Applied to the Desing of a Coal-Over-Coal Reburn Process at Vado Ligure Unit #4 (320 MWe)", Proceedings of the 4th International Symposium on Coal Combustion, Beijing, China, 18-25 August.

Coelho, P. J., 1999a, "Mathematical Modelling of the Convection Chamber of a Utility Boiler", Numerical Heat Transfer, Part A, Applications, Vol. 36(4), pp.411-428.

Coelho, P. J., 1999b, "An Engineering Model for the Calculation of Radiative Heat Transfer in the Convection Chamber of a Utility Boiler", Journal of the Institute of Energy, Vol. 72, pp.117-126.

Coimbra, C.F.M., Azevedo, J.L.T. and Carvalho, M.G., 1994, "3-D Numerical Model for Predicting NOx Emissions from a Pulverised Coal Industrial Boiler", FUEL, 73(7): 1128-1134.

Eaton, A.M., Smoot, L.D., Hill, S.C., e Eatough, C.N., 1999, "Components, Formulations, Solutions, Evaluation, and Application of Comprehensive Combustion Models", Progress in Energy and Combustion Science", Vol. 25, pp. 387-436.

EPRI, 1985, "Manual for Investigation and Correction of Boiler Tube Failures", Southwest Research Institute, EUA.

Bernardini, P.A.N., Furukawa, E., Bueno, E. , 1999, "Identificação de Causa de Fratura em Tubo de Superaquecedor Final da Caldeira No. 5 da UTLB", Relatório Técnico para Tractebel Energia, Universidade Federal de Santa Catarina.

Felippe, L. and Santo, E. O., 1998, "Caldeiras a Vapor – Análise dos Mecanismos de Falhas/Histórico e Tendências – Experiências na Usina Termelétrica Jorge Lacerda B – UTLB", Proceedings of the XV Seminário Nacional de Produção e Transmissão de Energia Elétrica, Foz do Iguaçu, Brazil.

Lockwood, F.C., 1981, and Shah, N.G., "A New Radiation Solution Method for Incorporation in General Combustion Prediction Procedures", Proceedings of the 18th Symposium on Combustion, The Combustion Institute, pp. 1405-1414.

Toledo, R., and Azevedo, J.L.T., 2003, "CDF Based Numerical Modeling of Different Furnace Configurations Using Air Staging and Reburning", This Conference.

Xu, M., Azevedo, J.L.T., e Carvalho M.G., 2000, "Modeling of the Combustion Process and NO_x Emission in a Utility Boiler", Fuel, Vol. 79, pp. 1611-1619.

Zukauskas, A., Skrinska, J., Ziugzda and Gnielinski, V. ,1998, "Single-Phase Convective Heat Transfer - Banks of Plain and Finned Tubes", Chap. 2.5.3 in 'Heat Exchanger Design Handbook', Ed. by G.F. Hewitt (Executive Editor), Begell House.

7. Aknowledgements

The authors thank CAPES and CNPq for providing a scholarship to R.F.Reinaldo, and CAPES and GRICES for the financial support to the international cooperation program between the Federal University of Santa Catarina (Brazil) and the Instituto Superior Tecnico (Portugal).